DESIGN AND SIMULATION OF SERIES LOADED RESONANT CONVERTER

Aizatul Azlin binti Ghazali

Faculty of Electrical Engineering,Universiti Teknologi MARA
40450, Shah Alam, MALAYSIA
akunick_14286@yahoo.com

***Abstract-* In this paper, design techniques and simulation of the series loaded resonant converter operating above resonance are presented. The half-bridge series loaded resonant topology is considered in this paper. This converter had been designed based on 100 kHz switching frequency with variation of input voltage of $50V \pm 20\%$. From the voltage conversion ratio, $\frac{Vo}{Vin}$ curve, the desired natural frequency, ω_o can be determined by approximate the value of ω_n which is 1.1. The value of resonant frequency f_o can be determined. The result shows that the tank circuit (L and C) is maintained in the continuous conduction mode which gives sinusoidal waveform. Detailed circuit simulation is carried out using PSIM simulation package to verify the circuit operation.**

I. INTRODUCTION

Resonant conversion techniques may be employed to achieve either DC to DC conversion for power supply applications or DC to high frequency AC power conversion, most commonly for induction heating [1]. Resonant converters (RCs) feature zero-voltage switching (ZVS), high frequency operation, high efficiency, small size, and lower electromagnetic interference [2].

Therefore, many new soft switching techniques such as zero voltage switching (ZVS) have been developed to reduce the component stresses of voltage and current and switching losses in the traditional Pulse-Width- Modulation converters.[3-7]

Among them, the partial series resonant DC/DC converters with low cost and suitable application in the kilowatt range have been studied by many researchers and designers [8-10] .

A resonant converter is a power supply topology that enables improved efficiency by introducing sinusoidal switching waveforms instead of the more commonly used square waveforms [11] . This causes the provision of Zero Voltage Switching (ZVS) modes. With this mode, the switch in the converter is turned on or off when the voltage across it is zero, thus the switching losses are minimized [12].

The central part of a converter is an L-C circuit, known as a tank circuit, which is maintained in continuous oscillation close to its natural frequency by the switching action of semiconductor devices; half and full-bridge configurations being most common. A DC output may be obtained by rectifying and smoothing either the resonant voltage or current. In this paper, the half bridge configuration had been used in the design and simulation [1].

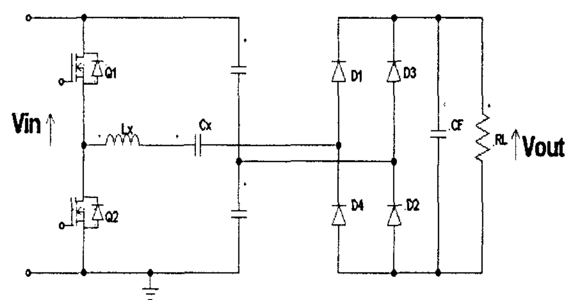

Fig 1. Half –bridge, series loaded resonant converter

The sine-wave approximation is based on the fact that the resonant tank current is approximately a sine wave for operation around the tank natural resonant frequency [13].

To produce the sinusoidal waveforms, the resonant converter utilizes an LC resonant tank circuit [14]. The proposed circuit can be operated above or below the resonant frequency of the resonant circuit. In order to avoid harmonics from occurs at the current of tank element the proposed circuit had been chosen to operate just above the resonant frequency [15].

In figure 2 waveforms are shown for a resonant converter operating above resonance. The fact that, the circuit is operating above resonance can be deduced from the fact that the current delivered to the resonant circuit (current in L) is lagging the voltage applied to the resonant circuit [3].

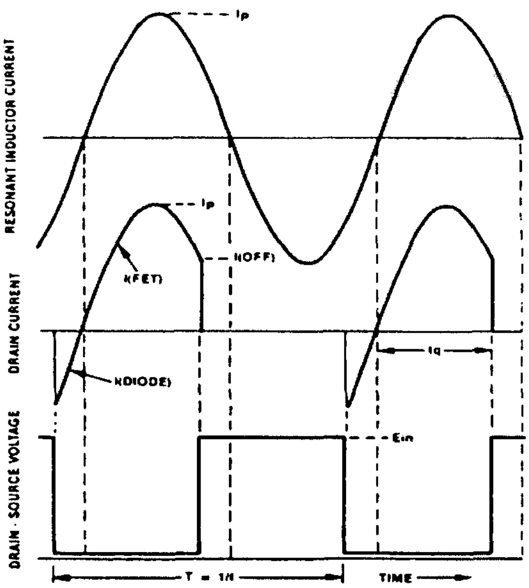

Fig 2. Ideal resonant converter waveforms.

II. THEORITICAL BACKGROUND OF SERIES LOADED RESONANT CONVERTER (SLR)

To examine the device currents and switching conditions in a resonant converter, the simplified circuit of figure is considered. A half-bridge network is shown driving a series L-C-R circuit. The transistors are operated at frequencies which close to the natural frequency of the L-C network. The resultant half-bridge output voltage, Vxy, is a square wave switching between $\pm\frac{Vin}{2}$ [1].

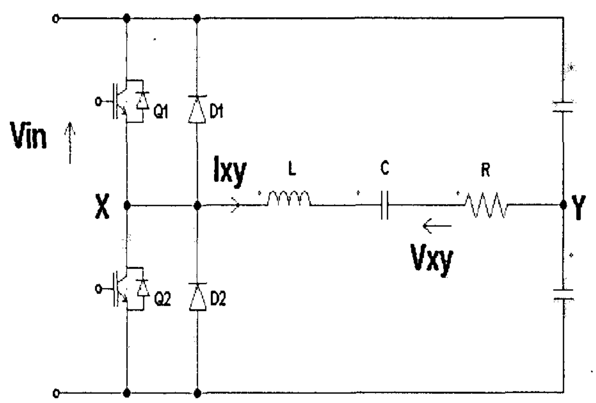

Fig. 3. Half-bridge and series L-C-R network.

The current in the L-C-R network is calculated by considering the square wave voltage impressed across the network as a Fourier series. The current flow due to each voltage component is obtained using the circuit impedance at the appropriate frequency, and the total current may be determined by superposition.

$$Z_{LCR} = L + C + R$$

$$= R + j\left[\omega L + \frac{1}{\omega C}\right]$$

$$= Z\left[\frac{1}{Q} + j\left(\frac{\omega_s}{\omega_o} - \frac{\omega_o}{\omega_s}\right)\right] \tag{1}$$

Where

Quality factor, Q Resonant factor, ω_o

$$Q = \frac{\omega_o L}{R} \tag{2}$$

$$\omega_o = \frac{1}{\sqrt{LC}} \tag{3}$$

In this converter the resonant current rather than the voltage, is rectified and smoothed to form the DC output and it is assumed that the MOSFET body diodes form the half-bridge anti-parallel diodes. Since the rectifier current is rectified, the output filter only consists of a shunt-connected capacitor [1,3].

A fundamental frequency equivalent circuit may be used to analyze the steady-state operating conditions of this converter. The converter voltage conversion ratio may then be determined:

$$\left|\frac{V_o}{V_{in}}\right| = \frac{1/2}{\left|1 + j\frac{\pi^2}{8}Q\left[\frac{\omega_s}{\omega_o} - \frac{\omega_o}{\omega_s}\right]\right|} \tag{4}$$

Q is again defined such that a low Q corresponds to heavy damping of the resonant tank. However, since the load is effectively in series with tank, a high value of load resistance corresponds to a heavy damping condition.

The voltage conversion ratio of the converter has been plotted against ωs/ωo that includes the magnitude of equation (4) with Q as parameter. The voltage conversion ratio is highly load dependent, but always less than 0.5.

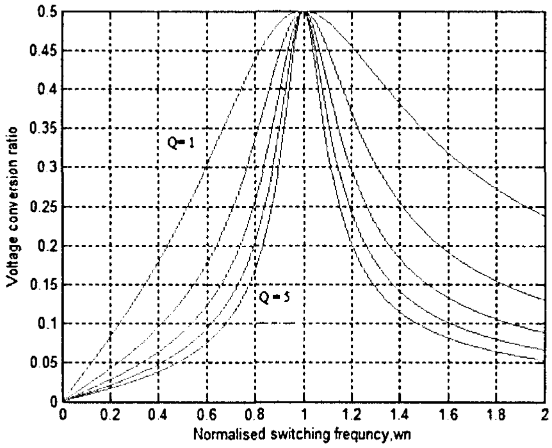

Fig. 4. Voltage conversion ratio for series-loaded resonant converter with Q = 1,2,3,4,5.

Small frequency variation in region of resonance may be used to control the converter; however, for low loads that are small values of Q, the conversion characteristics become insensitive to frequency changes. This suggests that the converter is unable to operate down to operate down to zero loads [1].

III. METHODOLOGY

A. First SLR Design

Figure 5 illustrates the design of SLR converter presented in this paper. The main parameter such as resonant frequency, component of tank circuit and switching frequency of 100kHz were each considered in the design. In the design, output power ($24<P_o<240$W), output current ($2 < I_o < 20$A) and output voltage (12V) ratings were chosen to be low enough, such that no transformer would be needed for the converter.

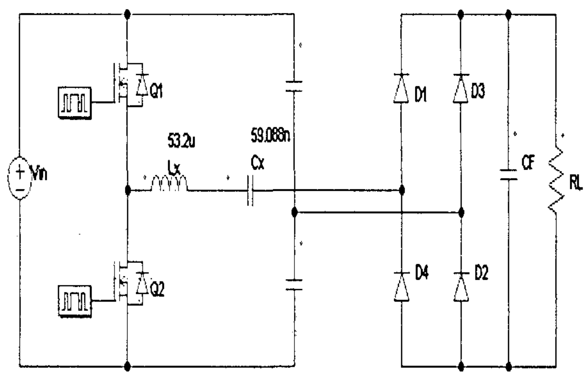

Fig. 5. Design circuit of SLR

The switching devices, which are MOSFETs Q1 and Q2, had been chosen based on their fast switching capability such that they can be switched up to 11MHz. The design was based on the quality factor, Q of 5 and 50V ±20% of input voltage which gives 40V and 60V respectively. The output voltage was to be design as 12V. The voltage gain, M can be calculated by using equation (5). The maximum and minimum voltage gain can be determined.

$$M = \left|\frac{V_o}{V_{in}}\right| \quad (5)$$

$$M_{max} = \left|\frac{12}{40}\right| = 0.3, \quad (6)$$

$$M_{min} = \left|\frac{12}{60}\right| = 0.2 \quad (7)$$

From the voltage conversion ratio curve obtained using MATLAB software, the point of $M_{max} = 0.3$ *was at* $\omega_n = 1.114$ and $M_{min} = 0.2$ was at ω_n =1.203 can be observed.

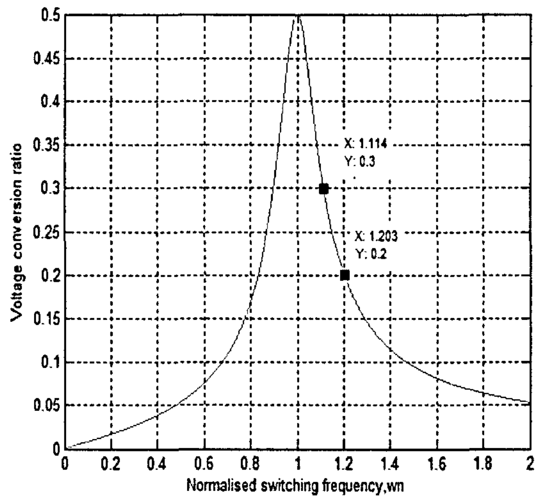

Fig. 6. Voltage conversion ratio curve at Q = 5.

In the first design, output current, I_o = 2A and Q = 5 had been used. The load resistor , R_l is 6Ω. By using 100 kHz as the switching frequency, f_s, resonant frequency, f_o can be calculated.

$$\omega_n = \frac{\omega_S}{\omega_o} \quad (8)$$

$$\omega_o = 2\pi f_o \quad (9)$$

From equation (6) and (7), the calculated value of ω_o is 564020.1975 and f_o is 89766.6Hz. This value was found at $M_{max} = 0.3$ *was and* $\omega_n = 1.114$. To find the value of tank circuit component, L and C, the natural frequency of tank circuit, ω_o at M_{min} must be same as ω_o at M_{max} which is 564020.1975.

Since the value of ω_o had been retained, new switching frequency must be obtained. At M_{min} = 0.2 and ω_n =1.203, new ω_S is 107989 Hz. Then, the value of L and C can be determined by using equation (2) and (3).

Find L

$$Q = \frac{\omega_o L}{R},$$

$$L = \frac{QR}{\omega_o}$$

$$= \frac{(5)(6)}{564020.1975}$$

$$L = 53.2\,\mu H \qquad (10)$$

Find C

$$\omega_o = \frac{1}{\sqrt{LC}},$$

$$C = \frac{\left(\frac{1}{\omega_o}\right)^2}{L}$$

$$= \frac{\left(\frac{1}{564020.1975}\right)^2}{53.2\,\mu H}$$

$$C = 59.088nF \qquad (11)$$

After these values had being obtained, the charging capacitor, C1 and C2 had been set to 10μF and C_F was set to be 100μF. These values had been plug in the design circuit shows in figure 5. Simulations by p-sim supersede this action.

Input voltage, Vin	Switching frequency, f_s
40 V	100 kHz
60 V	107.989 kHz

Table 1 : Switching frequency base on input voltage at Q =5.

B. Second SLR Design

In the second design, it focused on the output current of 20A but the some parameter such as input voltage, V_{in}, 50V $\pm 20\%$ and output voltage, V_o, 12V remain the same. The natural frequency of tank circuit, ω_o, the tank circuit element which is inductor, L and capacitor, C must fixed as the obtained value from the first design.

Parameter / Element	Value
Natural frequency of tank circuit, ω_o,	564020.1975
Inductor, L	53.2 μH
Capacitor, C	59.088nF

Table 2 : Value of remain parameter and element.

In this stage, the quality factor, Q was no longer equal to 5. Since the output current was changed, the value of load resistor, R_l = 0.6 Ω. The value of new Q can be obtained from equation (2). And a curve of new Q had been plotted.

New Quality Factor, Q

$$Q = \frac{\omega_o L}{R}$$

$$= \frac{(564020.1975)(53.2\,\mu)}{0.6}$$

$$= 50 \qquad (12)$$

From the voltage conversion ratio curve obtained using MATLAB software, the point of $M_{max} = 0.3$ *was at* $\omega_n = 1.011$ and M_{min} = 0.2 was at ω_n =1.019 can be observed.

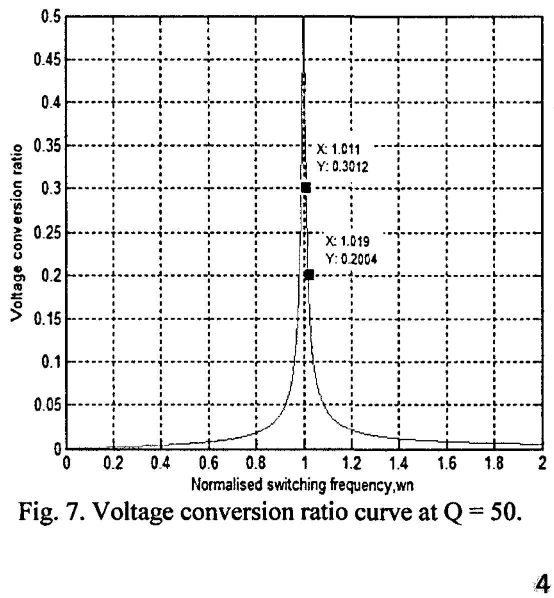

Fig. 7. Voltage conversion ratio curve at Q = 50.

In this stage, new switching frequency must obtained for both input voltage, V_{in}, 40V and 60V. This can be performed by using equation (6). At M_{max} = 0.3 *was and* $\omega_n = 1.011$, the new ω_S is :

$$\begin{aligned} \omega_S &= \omega_n\,\omega_o \\ &= (1.011)(564020.1975) \\ &= 570224.4197 \end{aligned} \tag{13}$$

Switching frequency, f_s

$$\begin{aligned} f_s &= \frac{\omega_S}{2\pi} \\ &= \frac{570224.4197}{2\pi} \\ &= 90754.035\,Hz \end{aligned} \tag{14}$$

At M_{min} = 0.2 *was and* $\omega_n = 1.019$, the new ω_S is:

$$\begin{aligned} \omega_S &= \omega_n\,\omega_o \\ &= (1.019)(564020.1975) \\ &= 574736.581 \end{aligned} \tag{15}$$

Switching frequency, f_s

$$\begin{aligned} f_s &= \frac{\omega_S}{2\pi} \\ &= \frac{574736.5813}{2\pi} \\ &= 91472.16788\,Hz \end{aligned} \tag{16}$$

Input voltage, Vin	Switching frequency, f_s
40 V	90754.035 Hz
60 V	91472.16788Hz

Table 3 : Switching frequency base on input voltage at Q = 50.

IV. SIMULATION RESULTS

The design described in the previous section, the SLR converter was simulated using PSIM. The complete schematic used in the PSIM was incorporating those values calculated from the design. The current and voltage waveform had been analyzed using time domain analysis. Basically, there are two designed circuit had been simulate. The difference between these two circuits is the output current which is 2A and 20A but the other parameter such as input voltage, V_{in}, 50V $\pm 20\%$ and output voltage, V_o, 12V remain the same. The switching frequency for circuit varies based on the operating band of the curve. (At Q = 5 and 50).

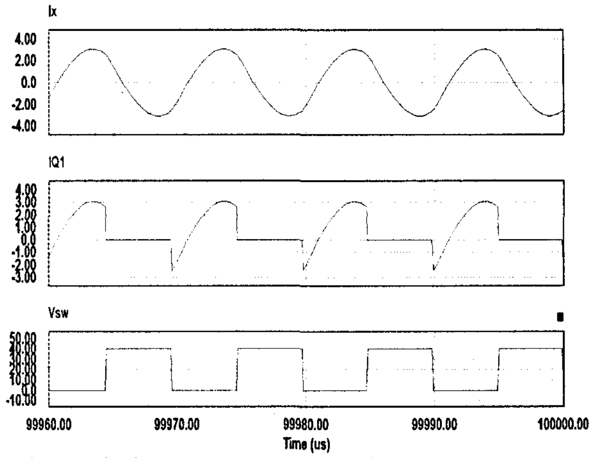

Fig. 8. Ideal resonant waveform of inductor current, drain current and switching voltage at frequency of 100 kHz from PSIM simulation.

Figure 8 shows that the waveforms of the inductor current drain current and switching voltage verify the theoretical parts of ideal resonant converter waveform.

A. Result for first SLR design

Basically, to simulate the first design circuit, the frequency was set to 100 kHz for V_{in} = 40V and 107.989 kHz at V_{in} = 60V. The objective of this simulation was to observe that the design circuit produced a sinusoidal waveform at the tank circuit element and also to achieve the desired output voltage and output current, which is 12V and 2A respectively.

Normalized switching frequency, ω_n	Theoretical value of switching frequency	Output voltage, V_o	Output current, I_o
ω_n = 1.114	100 kHz	11.16 V	1.859A
ω_n = 1.203	107.989 kHz	11.40V	1.900A

Table 4 : Theoretical value of switching frequency with the produced output..

At V_{in} = 40V, f_s= 100 kHz;

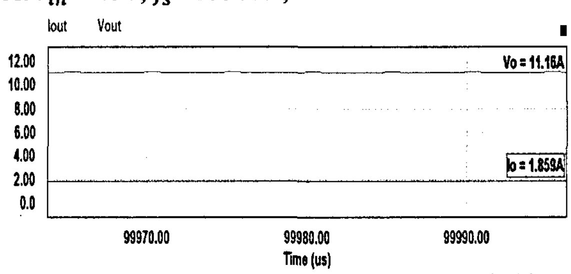

Fig. 9. Output voltage and output current at switching frequency of 100 kHz.

From figure 9, it can be clearly seen that, at the theoritical value of switching frequency, which is 100 kHz, did not achieved the desired ouput voltage and output current which is 12V and 2A respectivley.

In order to achieve the desired output, variations on the switching frequency had been done trough PSIM. The simulation value is 98550 Hz. This value produced the desired output.

Normalized switching frequency, ω_n	Theoretical value switching frequency	Simulation value switching frequency
$\omega_n = 1.114$	100 kHz	98550 Hz

Table 5 : Theoretical and simulation value of switching frequency.

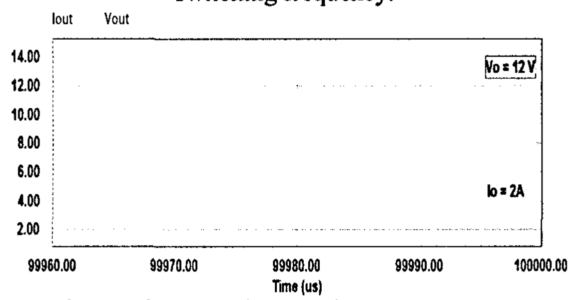

Fig. 10. Output voltage and output current at switching frequency of 98550 kHz.

Since, both output waveform in figure 9 and 10, were in a straight line and ripple less, it can be assumed that the operation is stable.

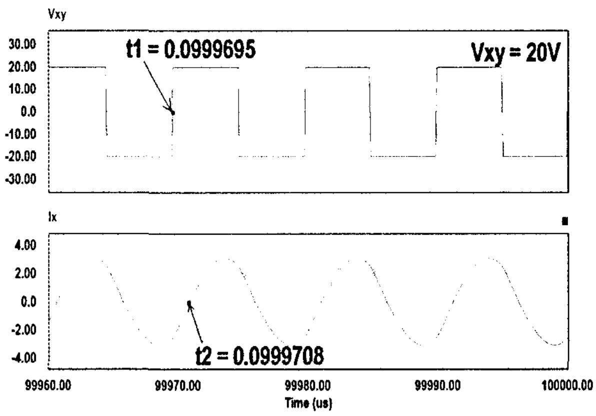

Fig. 11. Waveform of the voltage and current at the tank circuit element.

From the figure 11, the waveform of the Vxy equal to 20V. This verifies the theory that it is a square wave switching which resulting into $\pm\frac{Vin}{2}$. The waveform of the current also shows that, it is sinusoidal waveform due to the switching above the resonant frequency.

The switching angle or phase angle can be calculated using equation 17. From the observation, the total time taken for one cycle is $1.02\,X\,10^{-5}$s. From calculation switching angle for figure 11, $\theta_{DC-DC} = 45.88^o$.

$$\frac{\theta^o}{360^o} = \frac{\Delta T}{T}$$

$$\theta^o = \frac{\Delta T}{T}\ X\,360^o \qquad (17)$$

Where:

θ^o is a switching angle or phase angle
$\Delta T = t1 - t2$ Is a Time difference between point t1 and t2
T is a time taken for complete 1 cycle

At V_{in} = 60V, f_s= 107.989 kHz,

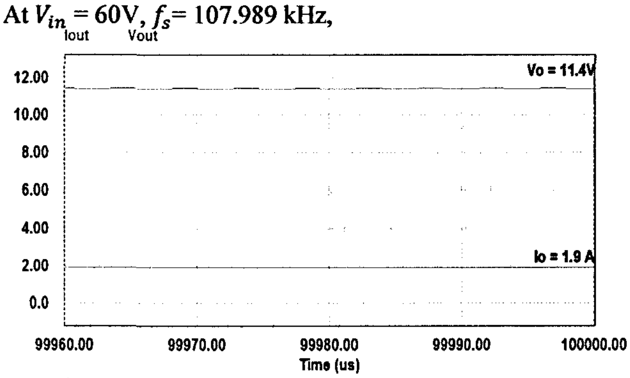

Fig. 12. Output voltage and output current at switching frequency of 107989 Hz.

In figure 12, it reflects the same thing as figure 9 in which the theoretical value of the switching frequency did not achieve the desired output.

In order to achieve the desired output, variations on the switching frequency had been done trough PSIM. The simulation value is 106800 Hz. This value produced the desired output.

Normalized switching frequency, ω_n	Theoretical value switching frequency	Simulation value switching frequency
ω_n =1.203	107.989 kHz	106800 Hz

Table 6 : Theoretical and simulation value of switching frequency.

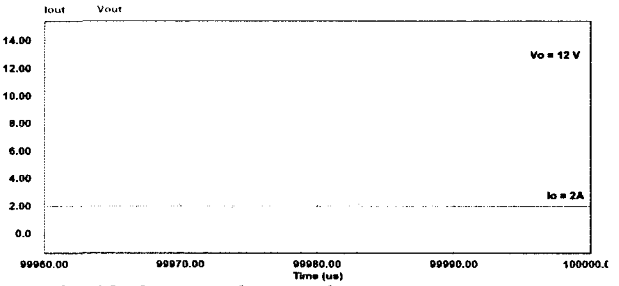

Fig. 13. Output voltage and output current at switching frequency of 106800 Hz.

Waveform in figure 13 also shows that the outputs is in a straight line and ripple less. Thus, it is in at stable condition.

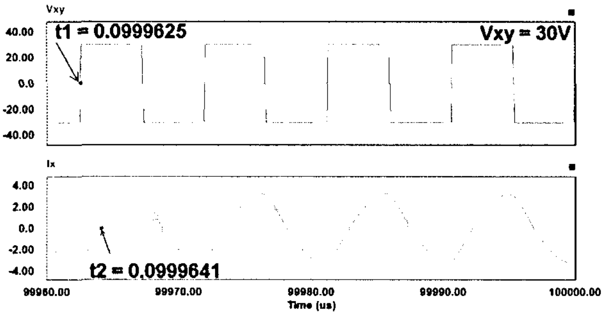

Fig. 14. Waveform of the voltage and current at the tank circuit element.

The straight line at figure 13, shows that the operation is stable. Figure 14 verify the theory at which the Vxy is equal to $\pm\frac{Vin}{2}$ which is 30V. The sinusoidal waveform of the current shows that it is operating above the resonant frequency.

The total time taken for one cycle is $9.4\,X\,10^{-6}$s. From calculation using equation 17 switching angle for figure 11, $\theta_{DC-DC} = 61.28^{o}$.

B. Results for second SLR design

In this stage, the frequency was set to 90754.03507 Hz for V_{in} = 40V and 91472.16788 kHz at V_{in} = 60V to achieve 20A output current and 12V output voltage.

Normalized switching frequency, ω_n	Theoretical value of switching frequency	Output voltage, V_o	Output current, I_o
ω_n = 1.011	90754.03507Hz	11.63 V	19.38A
ω_n = 1.019	91472.16788Hz	11.96V	19.94A

Table 7 : Theoretical value of switching frequency with the produced output.

At V_{in} = 40V, f_s= 90754.03507Hz;

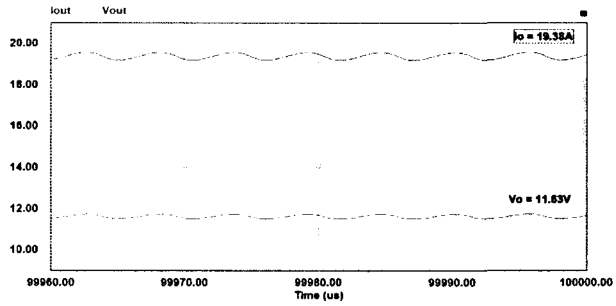

Fig. 15. Output voltage and output current at switching frequency of 90754.03507 Hz.

From figure 15, it can be clearly seen that the desired output was not achieve theoretical switching frequency. The theoretical value resulting in slightly lower from the desired output. From figure 15, the results is no longer in a straight line. The output had become more ripples.

$$\begin{aligned}\%\text{ of ripple voltage} &= \frac{\Delta Vo}{Vo} \times 100\% \\ &= \frac{0.37}{12} \times 100\% \\ &= 3.083\ \%\end{aligned} \quad (18)$$

From equation 18, it shows that the percentage of the ripple voltage is 3.083% from the desired output. When compared to the previous designed which had 0%, this indicate that, the operation is not stable.

In order to achieve the desired output, variations on the switching frequency had been done trough PSIM. The simulation value is 90690 Hz. This value produced the desired output.

Normalized switching frequency, ω_n	Theoretical value switching frequency	Simulation value switching frequency
ω_n = 1.011	90754.03507Hz	90690 Hz

Table 8 : Theoretical and simulation value of switching frequency.

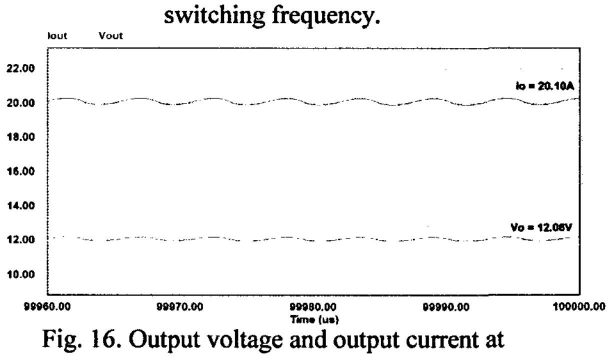

Fig. 16. Output voltage and output current at switching frequency of 90690 Hz.

From figure 16, it can be clearly seen that the desired output achieved by using switching frequency of 90690 Hz. The result is no longer in a straight line. The output had become more ripples.

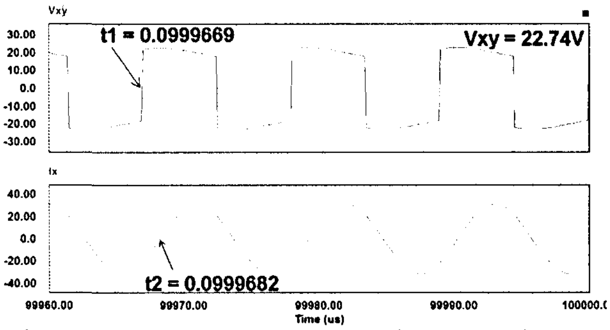

Fig. 17. Waveform of the voltage and current at the tank circuit element.

Figure 17 shows that the voltage waveform is in square wave and the current waveform is sinusoidal. This verifies the theory of square wave switching and switching above resonant frequency.

This verifies the theory at which the Vxy is equal to $\pm\frac{Vin}{2}$ which is 22.74V. Vxy is slightly changed from the pure square waveform. This is because of this design produced high current compared to the previous design.

From the observation, the total time taken for one cycle is $1.11\,X\,10^{-5}$s. From calculation using equation 17, the switching angle for figure 17, $\theta_{DC-DC} = 42.55^{o}$.

At V_{in} = 60V, f_s= 91472.16788 Hz ;

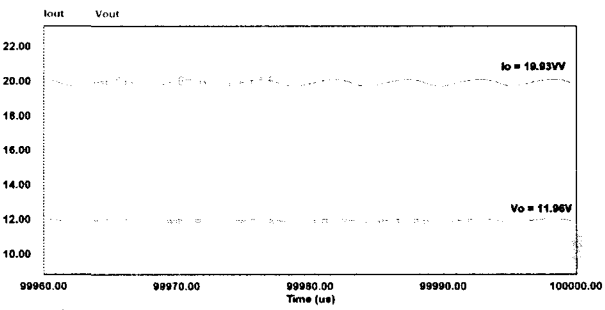

Fig. 18. Output voltage and output current at switching frequency of 91472.1688 Hz.

Figure 18, the simulation using the theoretical value of switching frequency did not achieve the desired output. The result is no longer in a straight line. The output had become more ripples.

$$\% \text{ of ripple voltage} = \frac{\Delta Vo}{Vo} \text{ x } 100\% \qquad (19)$$
$$= \frac{0.04}{12} \text{ x } 100\%$$
$$= 0.3333\%$$

From equation 19, in can be seen that the percentage of the ripple voltage is higher than at the input voltage is 40V, which have 0.3333% ripple, this indicate the operation are not stable.

In order to achieve the desired output, variations on the switching frequency had been done trough P-Sims. The simulation value is 91450 Hz. This value produced the desired output

Normalized switching frequency, ω_n	Theoretical value switching frequency	Simulation value switching frequency
$\omega_n = 1.011$	91472.1688 Hz	91450 Hz

Table 9 : Theoretical and simulation value of switching frequency

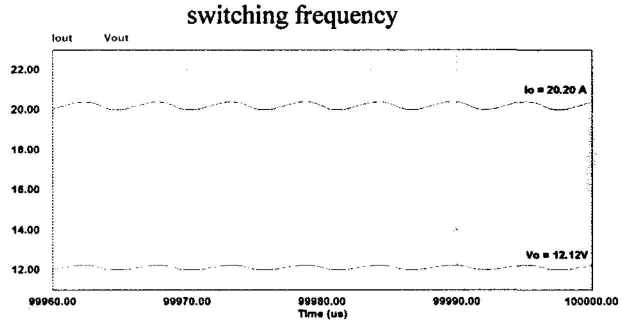

Fig. 19. Output voltage and output current at switching frequency of 91450 Hz.

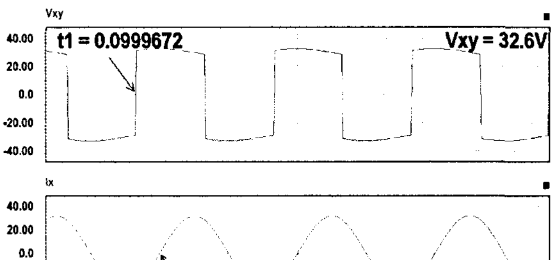

Fig. 20. Waveform of the voltage and current at the tank circuit element.

In figure 20, the voltage waveform is in square wave and the current waveform is sinusoidal. This verifies the theory of square wave switching and switching above resonant frequency.

This verifies the theory at which the Vxy is equal to $\pm\frac{Vin}{2}$ which is 32.6V. Vxy is slightly changed from the pure square waveform. This may because of this design produced high current compared to the previous design. From the observation, the total time taken for one cycle is $1.1\,X\,10^{-5}$s. From calculation using equation 17, the switching angle for figure 20 $\theta_{DC-DC} = 58.9^{o}$.

V. FLOW CHART

The flow of methodology used in this project is shown as below:

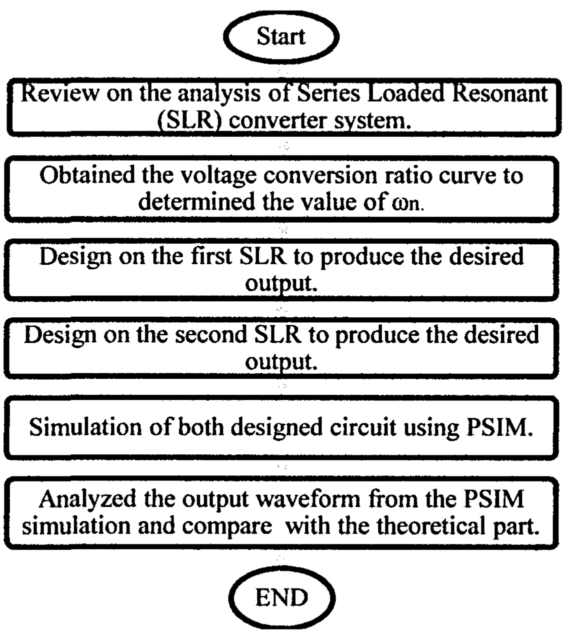

VI. FUTURE WORK

Generally, there were a few problems in getting the simulation to start. The initial condition such as the value of ω_n when voltage gain, M is equal to 0.2 and 0.3 must be found. In order to find these values, the voltage conversion ratio curve, $\frac{Vo}{Vin}$ must be obtained. Next problem deals with the design of the SLR itself. Instead of having an 12V of output voltage, the SLR were design to have a several range of the output current which is from 2A to 20A.

Future work on this SLR design and simulation could be include the method on how to control the output current range which can best describe as the closed loop system. The configuration of the full bridge SLR is the best way used to replace the half bridge configuration to increase the performance of the designed circuit.

VII. CONCLUSIONS

The design of series loaded resonant converter operating above resonant frequency had been presented. From the simulation, it shows that the current varies in proportion to the load current. This SLR in not suitable for high current applications due to the large output current related filter capacitor.

The theoretical calculation value was not tally with the simulation because, in the theoretical part, sine wave approximation was considered.

But in the simulation, the waveforms produced are slightly different from the sine wave approximation. This will also affect the switching angle, θ_{DC-DC} as well. This is because, in practical, the switching angle θ_{DC-DC} is in a range of $20^{o} < \theta_{DC-DC} < 30^{o}$. That is why the switching angle θ_{DC-DC} at the output waveform was out of range.

Besides that the theoretical calculation had helped much in doing the simulation. The comparison between theoretical results and simulation results had been showed.

VIII. ACKNOWLEDGEMENT

The author would like to thank her supervisor, Dr. Mohd Nawawi B Seroji for his support and knowledge on completing this paper.

REFERENCES

[1] M. A. cross, *et al.*, "High Frequency Power Electronic Circuits and Systems " in *MSc in Power Electronics and Drives, Module EE5B2*, ed: The University Of Birmingham, School of Electronic & ELectrical Engineering, 1998-1999.

[2] M. Borage, *et al.*, "Design of LCL-T Resonant converter Including The Effect of Transformer Winding Capacitance," *IEEE. Trans. Ind. Applicat.* , May 2009, pp. 1420-1427.

[3] R. L. Stegerwald, "A Comparison of Half-Bridge Resonant Converter Topologies," *IEEE. Trans. Power Electronics*, April 1998 pp. 174-182.

[4] J. A. Sabate, *et al.*, "Design Consideration for High-Voltage, High-Power, Full-Bridge Zero-Voltage Switched Pwm Converter.," presented at the IEEE-APEC Conf. Rec., 1990.

[5] M. K. Kazimierzuk, "Class-D Voltage Switching Mosfet Power Amplifier," *IEE Proc.*, November 1991, pp. 285-296.

[6] G. Hua, *et al.*, "An Improved Zero-Voltage Switched PWM Converter Using A Saturable Inductor," presented at the IEEE-PESC Conf. Rec., 1991.

[7] G. Hua, *et al.*, "Novel Zero Voltage Transition PWM Converter," presented at the IEEE-PESC Conf. Rec, 1993.

[8] P. C. Theron and J. A. Ferreira, "A new, Partial Series Resonant Converter for Efficient DC to DC Conversion," presented at the PCC-Yokohama, 1993.

[9] P. C. Theron and J. A. Ferreira, "The Zero Voltage Switching Partial Series Resonant Converter," *IEEE Trans. Ind Applicat.*, July / Aug 1995, pp. 879-886.

[10] M. A. D. Rooji, *et al.*, "A Novel Unity Power Factor Low - EMI Uninterruptible Power," *IEEE Trans. Ind. Applicat*, July /Aug 1998, pp. 870-876.

[11] R. W. Erikson and D. Maksimovic, *Fundamentals Of Power E.* Springer, 2001.

[12] S. D. Johnson, *et al.*, "Comparison of Resonant Topologies High-Voltage DC applications," in *IEEE Transcation on Aerospace and Electrronic System*, May 1998, pp. 263-274.

[13] R. L. Steigerwald, "Practical Design Methodologies For Load Resonant Converters Operating Above Resonance," pp. 172-178, 1992.

[14] M. McCarty, *et al.*, "Efficiency Perfomance Analysis of Series Loaded Resonant Converter," presented at the Symposium On Industrial Electronis and Applications (ISIEA 2009), Kuala Lumpur, Malaysia, 2009.

[15] C. F. *, *et al.*, "Design guidelines of the series resonant converter for very low current or very high frequency applications," presented at the 35th Annual IEEE Power Electronics Specialists Conference, Aachen, German, 2004.